

Article

Influence of Transition Metal on the Hydrogen Evolution Reaction over Nano-Molybdenum-Carbide Catalyst

Meng Chen ¹, Yufei Ma ^{1,*}, Yanqiang Zhou ¹, Changqing Liu ¹, Yanlin Qin ¹, Yanxiong Fang ¹, Guoqing Guan ², Xiumin Li ³, Zhaoshun Zhang ⁴ and Tiejun Wang ¹

¹ Department of Chemical Engineering, School of Chemical Engineering and Light Industry, Guangdong University of Technology, Guangdong 510006, China; chenmeng588254@126.com (M.C.); zhouyanqiang00@163.com (Y.Z.); clarkcqliu@163.com (C.L.); yllqin@gdut.edu.cn (Y.Q.); fangyx@gdut.edu.cn (Y.F.); tjwang@gdut.edu.cn (T.W.)

² Energy Conversion Engineering Group, Institute of Regional Innovation (IRI), Hirosaki University, 2-1-3 Matsubara, Aomori 030-0813, Japan; guan@hirosaki-u.ac.jp

³ School of Materials Science and Engineering, Zhengzhou University, Zhengzhou 450001, China; xiuminli0516@zzu.edu.cn

⁴ School of Chemistry and Chemical Engineering, Qufu Normal University, Qufu 273100, China; zhangzhaoshun@foxmail.com

* Correspondence: yufeima@gdut.edu.cn; Tel.: +86-020-3932-2237

Received: 29 June 2018; Accepted: 20 July 2018; Published: 22 July 2018



Abstract: The highly efficient electrochemical hydrogen evolution reaction (HER) provides a promising way to solve energy and environment problems. In this work, various transition metals (Fe, Co, Ni, Cu, Ag, and Pt) were selected to support on molybdenum carbides by a simple organic-inorganic precursor carburization process. X-ray diffraction (XRD) analysis results indicated that the β -Mo₂C phase was formed in all metal-doped samples. X-ray photoelectron spectroscopy analysis indicated that the binding energy of Mo²⁺ species (Mo₂C) shifted to a lower value after metal was doped on the molybdenum carbide surface. Comparing with pure β -Mo₂C, the electrocatalytic activity for HER was improved by transition metal doping on the surface. Remarkably, the catalytic activity improvement was more obvious when Pt was doped on molybdenum carbide (2% Pt-Mo₂C). The 2% Pt-Mo₂C required a η_{10} of 79 mV, and outperformed that of pure β -Mo₂C (η_{10} = 410 mV) and other transition metal doped molybdenum carbides, with a small Tafel slope (55 mV/dec) and a low onset overpotential (32 mV) in 0.5 M H₂SO₄. Also, the 2% Pt-Mo₂C catalyst demonstrated a high stability for the HER in 0.5 M H₂SO₄. This work highlights a feasible strategy to explore efficient electrocatalysts with low cost via engineering on the composition and nanostructure.

Keywords: hydrogen evolution reaction; nano-molybdenum-carbide; electro-catalysis; transition metal

1. Introduction

To solve environmental and energy problems, development of alternatively clean energy technology is becoming more and more important over the past several decades. Hydrogen is considered as a promising clean and flexible energy carrier and is expected to play a key role in future sustainable energy [1–4]. Energy from renewable sources such as sunlight and wind can be stored into the H₂ molecular chemical bond via water electrolysis, which then can be released through the reverse process in fuel cells on demand [5]. Several processes such as hydrocarbon reforming, and the water gas shift reaction have been applied to extract a hydrogen atom from traditional compounds such as

diesel, gasoline, methane, and methanol [6–10]. Among those processes, the directly electrochemical splitting of water into H₂ (Hydrogen Evolution Reaction, HER) is a promising way for hydrogen production. Crucial to enabling an energy-efficient splitting of water is the development of active and durable electrocatalysts for the HER reaction, and the electrocatalyst should work at the potential close to the HER thermodynamic value ($2\text{H}^+ + 2\text{e}^- \rightarrow \text{H}_2$; (0.198 + 0.059 pH) V versus normal H₂ electrode at 298 K) [11]. A noble metal catalyst (such as platinum) is well recognized as the best catalyst for the HER, requiring negligible overpotential to achieve reaction rate. However, due to the high cost and scarcity, platinum is severely limited in the widespread application in H₂ production through HER. Currently, the commercial HER catalyst is Pt-C. However, the Pt mass loading amount is usually over 20% [12,13]. Therefore, the currently crucial issue for an electrolytic conversion system is to explore efficient non-precious metal catalysts that are cheap and earth abundant or otherwise to sharply decrease the Pt loading amount in the current catalyst system [14,15].

Recently, transition metal carbides such as tungsten and molybdenum carbides have attracted much attention because they show catalytic activities similar to those of noble metals in various catalytic reactions such as the hydrogenation reaction, hydrocarbon isomerization, methanol steam reforming, water gas shift reaction, CO₂ reduction, and HER [7,10,16–21]. Vrabel and Hu found that Mo₂C nanoparticles showed excellent catalytic performance in HER [21]. Liu and Girault et al. synthesized molybdenum carbide nanowires by pyrolysis of a MoO_x/amine hybrid precursor with sub-nanosized periodic structure, and found that the high activity of molybdenum carbide nanowire was resulted from the enriched nano-porosity and large reactive surface. Compared with Mo₂C synthesized by the traditional process (e.g., temperature program carburization under CH₄/H₂ atmosphere), the nano-structured Mo₂C showed superior HER activity with lower onset overpotential and higher current densities [20]. Gao and Tang et al. synthesized the Co-doped Mo₂C nanowires by a facile Co-modified MoO_x-amine precursor, which also showed higher activity and stability for HER. The Co-Mo₂C nanowire with an optimal Co/Mo ratio of 0.02 displayed a low overpotential ($\eta_{10} = 140$ and 118 mV for reaching a current density of -10 mA/cm^2 ; $\eta_{100} = 200$ and 195 mV for reaching a current density of -100 mA/cm^2 in 0.5 M H₂SO₄ and 1.0 M KOH, respectively). They considered that this high catalytic performance was resulted from the effective Co inserting into the molybdenum carbide crystal structure, which increased the Mo₂C surface electron density around the Fermi level, resulting in the reduced strength of Mo-H for facilitated HER kinetics [22].

Our previous works demonstrated that supported transition metal nanoparticles (with lower loading amount, e.g., 2% or 5%) could dramatically affect the molybdenum carbide surface properties such as electron density or surface nano-structure, and these catalysts showed different catalytic performances in gas-solid reactions such as methanol steam reforming, the water gas shift reaction, and the formic acid decomposition reaction [7,8,10,23,24]. With increase in metal loading amount, the interaction between ad-metal and molybdenum carbide substrate will be weakened. On the other hand, the surface area could be decreased sharply in the case of a high metal loading amount. Herein, transition metal (Fe, Co, Ni, Cu, Ag, or Pt) doped nanowire molybdenum carbide (with lower doping amount) was synthesized via a facile method and used for the HER. Its electrocatalytic activity and stability were investigated and compared with pure Mo₂C. To understand the relationship between catalyst surface properties and electrocatalytic performance, the catalysts were characterized by X-ray diffraction (XRD), Brunner–Emmet–Teller measurements (BET), X-ray photoelectron spectroscopy (XPS), Scanning electron microscope (SEM), Transmission electron microscope (TEM), High-resolution TEM (HR-TEM) and inductive coupled plasma (ICP).

2. Results and Discussions

2.1. Characterization of as-Prepared Catalysts

A series of transition metal doped nano-wire molybdenum carbide (M-Mo₂C) samples were fabricated via annealing of metal (M) doped MoO_x/organic precursors under an Ar flow at 800 °C.

The crystal structure was determined by X-ray diffraction (XRD) analysis. Figure 1 shows XRD patterns of β - Mo_2C and various transition metal doped molybdenum carbide catalysts. The peaks at 2θ of 34.8° , 38.4° , 39.8° , 52.5° , 61.9° , 69.6° , and 74.9° are attributed to the presence of hexagonal β - Mo_2C (hcp crystal structure). The peak at 2θ of 40.5° is attributed to metallic Mo. No peaks corresponding to molybdenum oxides and metallic ferrum, cobalt, nickel, copper, silver, and platinum were observed. As shown in Figure 1, using the present method, when transition metal (Fe, Co, and Ag) precursors were applied, metallic Mo was formed in the final catalysts during the annealing process. However, in the cases of the doping of Pt, Ni, and Cu, no metallic Mo peak was observed. In general, the organic precursor of aniline is decomposed to CO, CH_4 , NH_3 , and H_2 at the high annealing temperature. Under the reducing atmosphere (CO, CH_4 , NH_3 , and H_2), the molybdenum carbide surface could be catalytically reduced by supported transition metal nanoparticles (e.g., Fe and Co) to metallic Mo. The 101 peak of Mo_2C in the XRD patterns ($2\theta = 39.8^\circ$) at various metal doped molybdenum carbides and β - Mo_2C are shown in the inserted figure in Figure 1. It can be found that compared with pure β - Mo_2C , the 101 peak of Mo_2C showed a slight shift to the lower diffraction angle. This indicated that during the annealing process, the doping transition metal atoms might be replaced by some Mo atoms in molybdenum carbide surface or inserted into the molybdenum carbide phase. The interaction between doping metal and molybdenum carbide substrate could vary the electron feature of Mo.

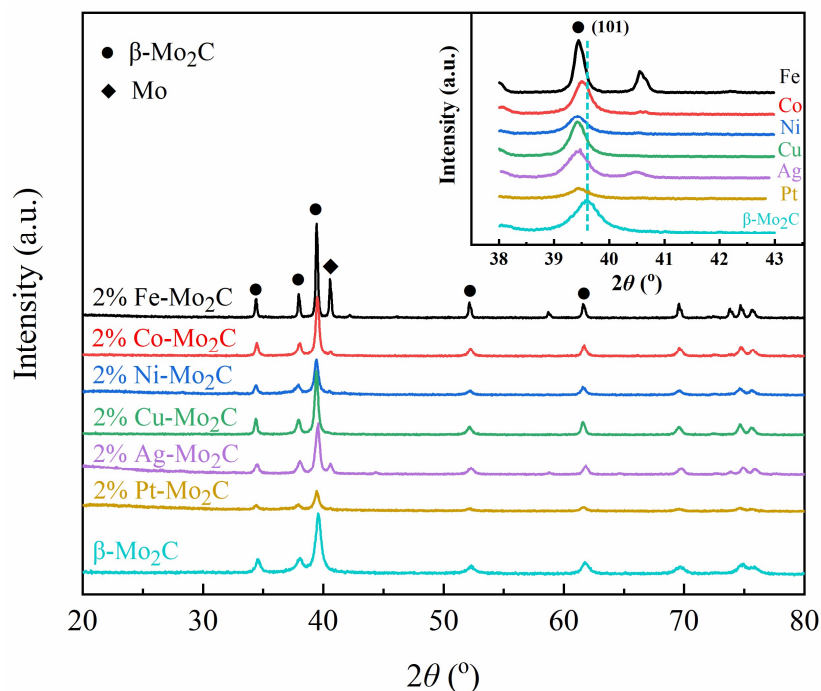


Figure 1. X-ray diffraction (XRD) patterns of various metal doped molybdenum carbides and pure β - Mo_2C .

To investigate the interaction between various doping transition metals and molybdenum carbide in more details, Mo 3d spectra of various metal doped molybdenum carbides (2% M- Mo_2C) and the pure β - Mo_2C were measured by XPS. As shown in Figure 2 (the XPS spectra of pure β - Mo_2C is not shown in this paper), the doublet peaks have a splitting of ~ 3.13 eV and a Mo $3d_{5/2}$ to Mo $3d_{3/2}$ ratio of 3:2. Meanwhile, the binding energy of the corresponding Mo $3d_{5/2}$ peak was obtained and is summarized in Table 1. By means of deconvolution, the carbide states distribution of the as-prepared catalyst surface can be estimated. There are four molybdenum species for 2% Ni- Mo_2C , 2% Cu- Mo_2C , and 2% Pt- Mo_2C catalysts: the one with Mo $3d_{5/2}$ binding energy (BE) of 228.0–228.6 is attributed to the Mo^{2+} species involved in Mo-C bonding (Mo_2C); three others with Mo $3d_{5/2}$ binding energy of 228.9–229.3, 230.6–232.2, and 232.3–233.3 are identified as Mo^{4+} (MoO_2), $\text{Mo}^{\delta+}$ (MoO_xC_y), and Mo^{6+}

(MoO_3), respectively. The δ is the intermediate oxidation state between 4 and 6 ($4 < \delta < 6$). The existence of molybdenum oxide should be attributed to the surface oxide formed during the passivation process. It should be noted that, for 2% Fe- Mo_2C , 2% Co- Mo_2C and 2% Ag- Mo_2C catalysts, not only the above four molybdenum species (e.g., Mo_2C , MoO_2 , MoO_xC_y and MoO_3) were found, but also metallic Mo was detected by XPS. The Mo $3d_{5/2}$ binding energy (BE) of 228.0, 228.1, and 228.1 were identified as metallic Mo species in 2% Fe- Mo_2C , 2% Co- Mo_2C and 2% Ag- Mo_2C catalysts surface, respectively. This observation is consistent with the previous XRD result. Regarding the consistent binding energy of the molybdenum oxide species and metallic species, it can be considered that the binding energy of Mo^{2+} species, e.g., Mo_2C , should be affected by the transition metal doping, which are the active species for electrocatalytic HER [25,26]. For the pure β - Mo_2C sample, the Mo $3d_{5/2}$ binding energy (BE) at 228.6 eV presents the Mo^{2+} species. By contrast, these peaks for Mo^{2+} are obviously shifted to the lower binding energy in the transition metal doping molybdenum carbide catalyst surface, in which the Pt doping leads to the lower binding energy (228.0 eV), indicating the enriched electrons around the Mo atom. This indicates that the doping metal affected the molybdenum carbide surface electron density structure. For the catalytic reaction, the catalyst surface electron density structure and surface nano-structure always play a crucial role, which can influence the catalytic activity and selectivity.

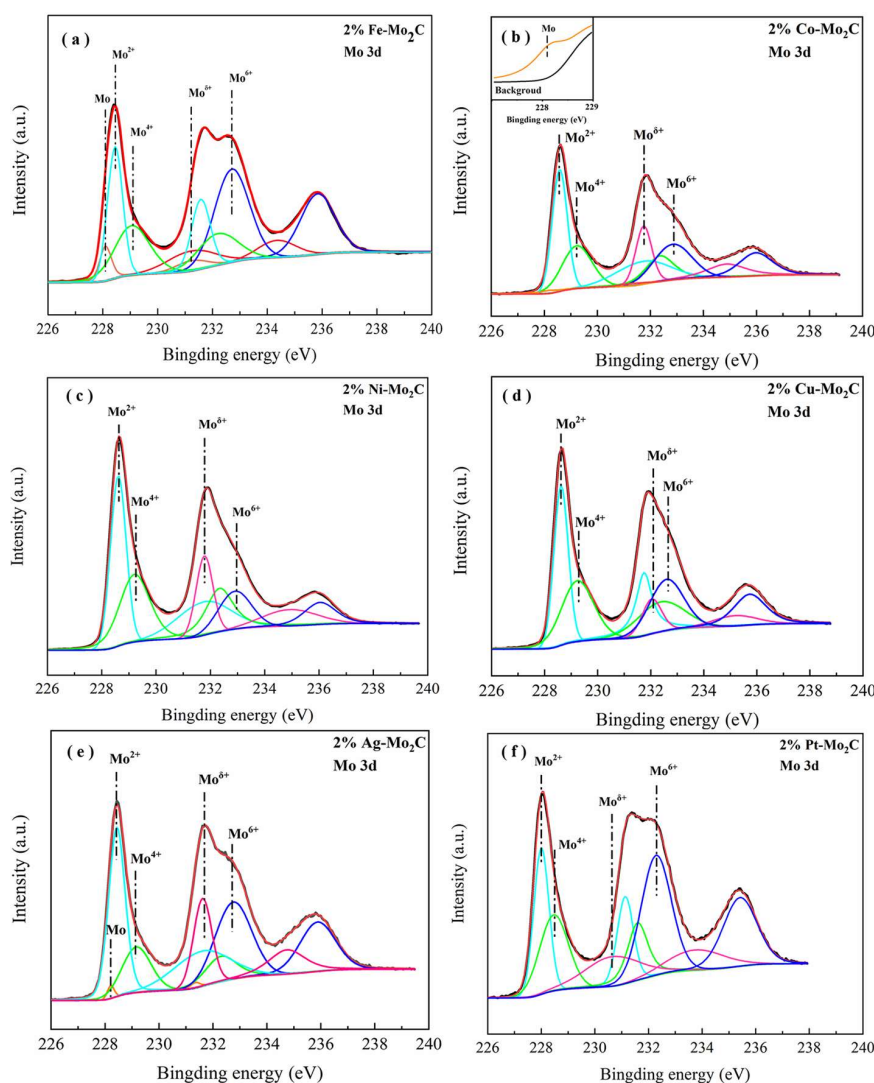


Figure 2. XPS spectra of (a) 2% Fe- Mo_2C , (b) 2% Co- Mo_2C , (c) 2% Ni- Mo_2C , (d) 2% Cu- Mo_2C , (e) 2% Ag- Mo_2C and (f) 2% Pt- Mo_2C .

Table 1. Mo 3d_{5/2} binding energy of 2% Fe-Mo₂C, 2% Co-Mo₂C, 2% Ni-Mo₂C, 2% Cu-Mo₂C, 2% Ag-Mo₂C, 2% Pt-Mo₂C and pure β-Mo₂C catalyst.

Catalysts	Mo 3d _{5/2} (eV)				
	Mo ²⁺ (Mo ₂ C)	Mo ⁴⁺ (MoO ₂)	Mo ^{δ+} (MoO _x C _y)	Mo ⁶⁺ (MoO ₃)	Mo ⁰ (Mo)
β-Mo ₂ C	228.60	229.30	232.20	233.30	-
2% Fe-Mo ₂ C	228.40	229.10	231.60	232.70	228.00
2% Co-Mo ₂ C	228.50	229.20	231.70	232.80	228.10
2% Ni-Mo ₂ C	228.58	229.20	231.80	232.90	-
2% Cu-Mo ₂ C	228.58	229.20	232.00	232.60	-
2% Ag-Mo ₂ C	228.40	229.10	231.60	232.70	228.20
2% Pt-Mo ₂ C	228.00	228.90	230.60	232.30	-

The standard deviation of Mo 3d_{5/2} binding energy (BE) was less than 0.1 eV.

The BET surface areas of pure β-Mo₂C and various metals doped molybdenum carbide catalysts are summarized in Table 2. It can be found that comparing to the pure β-Mo₂C, the surface area decreased sharply when Fe and Co was doped. It is possible that the Fe and Co nanoparticles could block some micro-structure pores during the synthesis process. This can be demonstrated from the measured pore size results as shown in Table 2. One can find that comparing with pure β-Mo₂C catalyst, the average pore size increasing sharply when Fe and Co were doped. This indicates that the smaller size pores were blocked by the doped Fe and Co nanoparticles. For 2% Ni-Mo₂C, 2% Cu-Mo₂C, and 2% Ag-Mo₂C, the surface areas decreased to some extent when the metal was doped. Relating to the average pore size results, the same reasons can be deduced as above mentioned (e.g., for 2% Fe-Mo₂C and 2% Co-Mo₂C). Notably, from the Table 2, it can be observed that compared with pure β-Mo₂C, the surface area was increased from 20.7 to 48.3 m²/g while the average pore size was decreased from 16.3 to 3.0 nm. The high surface area of 2% Pt-Mo₂C might be due to the high dispersion of Pt nanoparticles which cannot block the micro-structure pores. On the other hand, the crystalline sizes of Mo₂C were approximately 18.59 nm and 25.6 nm for 2% Pt-Mo₂C and 2% Fe-Mo₂C, respectively, calculated by using Scherrer's equation based on the 101 peak of Mo₂C shown in Figure 1. The smaller nanoparticle size of Mo₂C also could result in the higher surface area. Generally, the higher surface area indicates more catalytically active site exposure. The Co/Mo, Ag/Mo, and Pt/Mo molar ratios in metal doped molybdenum carbide are determined by inductively coupled plasma (ICP) as shown in Table 2. For other metals (e.g., Fe, Ni, and Cu) the signal cannot be detected by ICP. This might be due to much less metal atom doped into the molybdenum carbide phase during the synthesis process.

Table 2. Brunner–Emmet–Teller measurements (BET) surface area and inductive coupled plasma (ICP) of various metal doped molybdenum carbides and β-Mo₂C.

Catalyst	M/Mo ^a	Specific Surface Area (m ² /g)	Pore Volume (cm ³ /g)	Average Pore Size (nm)
β-Mo ₂ C	\	20.7	0.09	16.3
2% Fe-Mo ₂ C	\	3.2	0.01	50.7
2% Co-Mo ₂ C	0.5	9.7	0.06	44.1
2% Ni-Mo ₂ C	\	15.3	0.08	33.4
2% Cu-Mo ₂ C	\	14.9	0.07	19.9
2% Ag-Mo ₂ C	1.9	14.3	0.1	32.9
2% Pt-Mo ₂ C	0.2	48.3	0.06	3.0

^a M: Fe, Co, Ni, Cu, Ag, and Pt. Data calculated from ICP results.

The morphology of as-prepared catalyst was confirmed using SEM technology. Figure 3 shows the SEM images of various metal doped molybdenum carbides. They clearly indicate that different doped transition metals lead to distinct particle shapes and sizes. As shown in Figure 3a, Mo₂C doped

by Fe had a random morphology, and obviously agglomerated. In contrast, other metals (Co, Ni, Cu, Ag, and Pt) doped molybdenum carbide catalysts show wire-like morphology. On the other hand, one can see that small particles are attached on the molybdenum carbide wire surface for Co, Ni, Cu, Ag, and Pt doped molybdenum carbide catalysts. The small particles were of Mo_2C which were formed during the synthesis process. Based on the SEM results (see in Figure 3b–f), one can see that the wire diameter is about 50–100 nm with a length of about 1–3 μm .

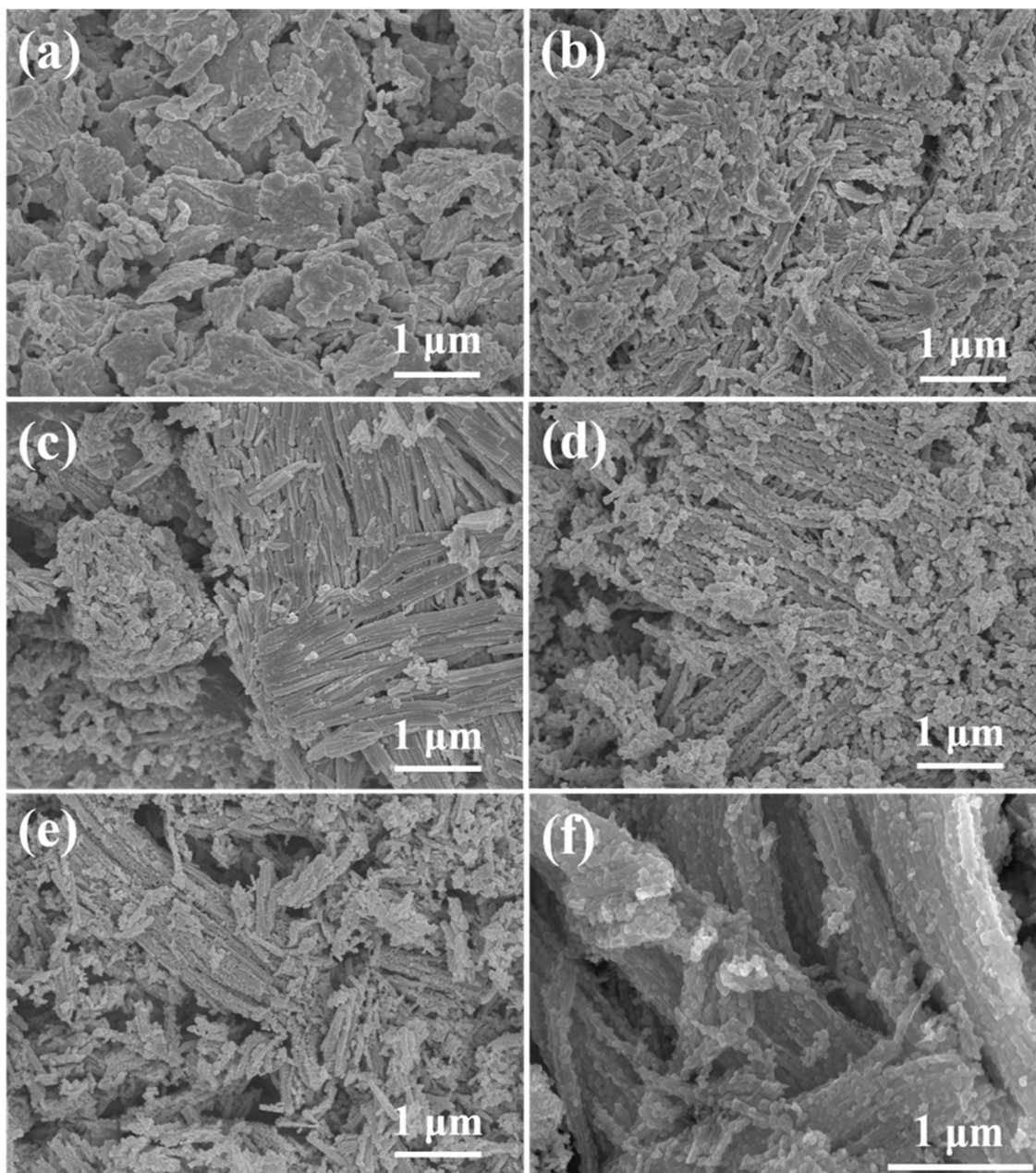


Figure 3. SEM images of various metal doped molybdenum carbide catalysts (a) 2% Fe- Mo_2C ; (b) 2% Co- Mo_2C ; (c) 2% Ni- Mo_2C ; (d) 2% Cu- Mo_2C ; (e) 2% Ag- Mo_2C ; (f) 2% Pt- Mo_2C .

Taking 2% Pt- Mo_2C as the model sample, the nanostructure was analyzed by scanning electron microscopy (SEM) as well as transmission electron microscopy (TEM). As shown in the Figure 4a,b the wire-like morphology can be clearly observed with the nanoparticles on the wire surface. The nanoparticle sizes in 100–200 nm is observed in Figure 4c. The TEM (Figure 4d) image further

displays that such a wire-like molybdenum carbide is composed by nanoparticles (the particle size is about 3–10 nm). The small particle size should result in high surface area and more active sites. The (101) and (002) lattice fringes with the interplanar spacing of 0.221 and 0.232, respectively, of β -Mo₂C are identified in the high-resolution TEM (HR-TEM, Figure 4e). The absence of a platinum nanostructure in the TEM and HR-TEM image is consistent with the XRD results. Furthermore, the energy dispersive spectrum (EDS) of 2% Pt-Mo₂C confirmed the main composition of Mo, Pt, and C (the results not shown in this paper [8]). Scanning transmission electron microscopy (STEM) and corresponding elemental mapping (Figure 4g) clearly show the uniform distribution of Mo and Pt elements (due to the fact that a carbon film was used in the TEM investigation, C element was not detected in this study), indicating the homogeneous Pt-doping into molybdenum carbide. Analogously, other samples (pure β -Mo₂C and Fe, Co, Ni, Cu, Ag doping molybdenum carbides) composed of well-defined nanoparticles were also observed by TEM analysis.

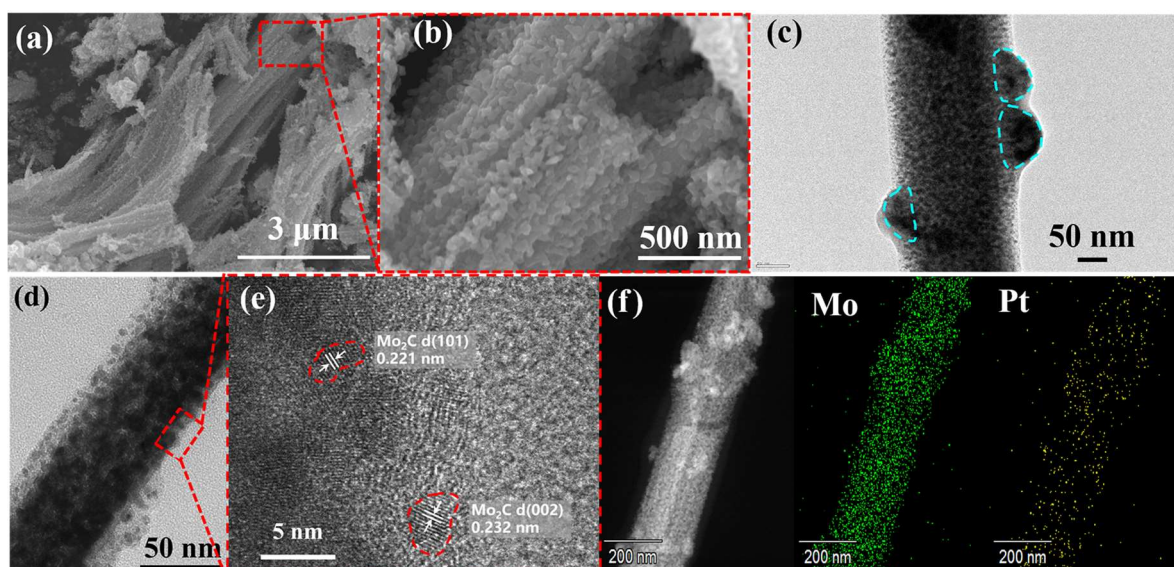


Figure 4. (a) and (b) SEM, (c) TEM, (d) TEM and (e) HR-TEM of 2% Pt-Mo₂C catalyst, and (f) the STEM image and the corresponding elemental mapping.

2.2. HER Catalytic Performance of Various Metal Doped Catalysts

To investigate the HER catalytic performance in an acidic electrolyte, the as-prepared pure β -Mo₂C and various metal doped molybdenum carbide catalysts were loaded onto glassy carbon electrodes (GCEs) with a mass loading of 0.272 mg/cm². Figure 5a displays their polarization curves with IR-drop correction in 0.5 M H₂SO₄, along with that of the commercial 20% Pt/C catalyst for reference. The HER activities of pure β -Mo₂C and various metals doped molybdenum carbide catalysts in 0.5 M H₂SO₄ are summarized in Table 3. The commercial 20% Pt/C catalyst shows a high HER activity, featured by a low overpotential (η_{10}) of 34 mV for reaching a current density ($-j$) of -10 mA/cm². In contrast, the wire-like molybdenum carbide catalyst showed a low HER activity, featured by a high overpotential (η_{10}) of 410 mV for reaching a current density ($-j$) of -10 mA/cm². However, the HER catalytic activity was obviously improved by doping transition metal onto the molybdenum carbide surface. The 2% Fe-Mo₂C, 2% Co-Mo₂C, 2% Ni-Mo₂C, 2% Cu-Mo₂C, and 2% Ag-Mo₂C required η_{10} of 377, 243, 205, 227, and 210 mV, respectively, lower than that of pure β -Mo₂C ($\eta_{10} = 410$ mV). Remarkably, the catalytic activity improvement was more obvious for Pt doped molybdenum carbide catalyst (2% Pt-Mo₂C). One can see that the 2% Pt-Mo₂C required a η_{10} of 79 mV, outperforms that of pure β -Mo₂C and other transition metal doped molybdenum carbides. Although this HER activity for 2% Pt-Mo₂C catalyst is still lower than the commercial 20% Pt/C catalyst, the economic cost (the

Pt loading amount in as-prepared 2% Pt-Mo₂C catalyst is much less than the commercial 20% Pt/C catalyst) and the earth-abundance of Mo metal highlights its promising prospect as a highly efficient HER electrocatalyst.

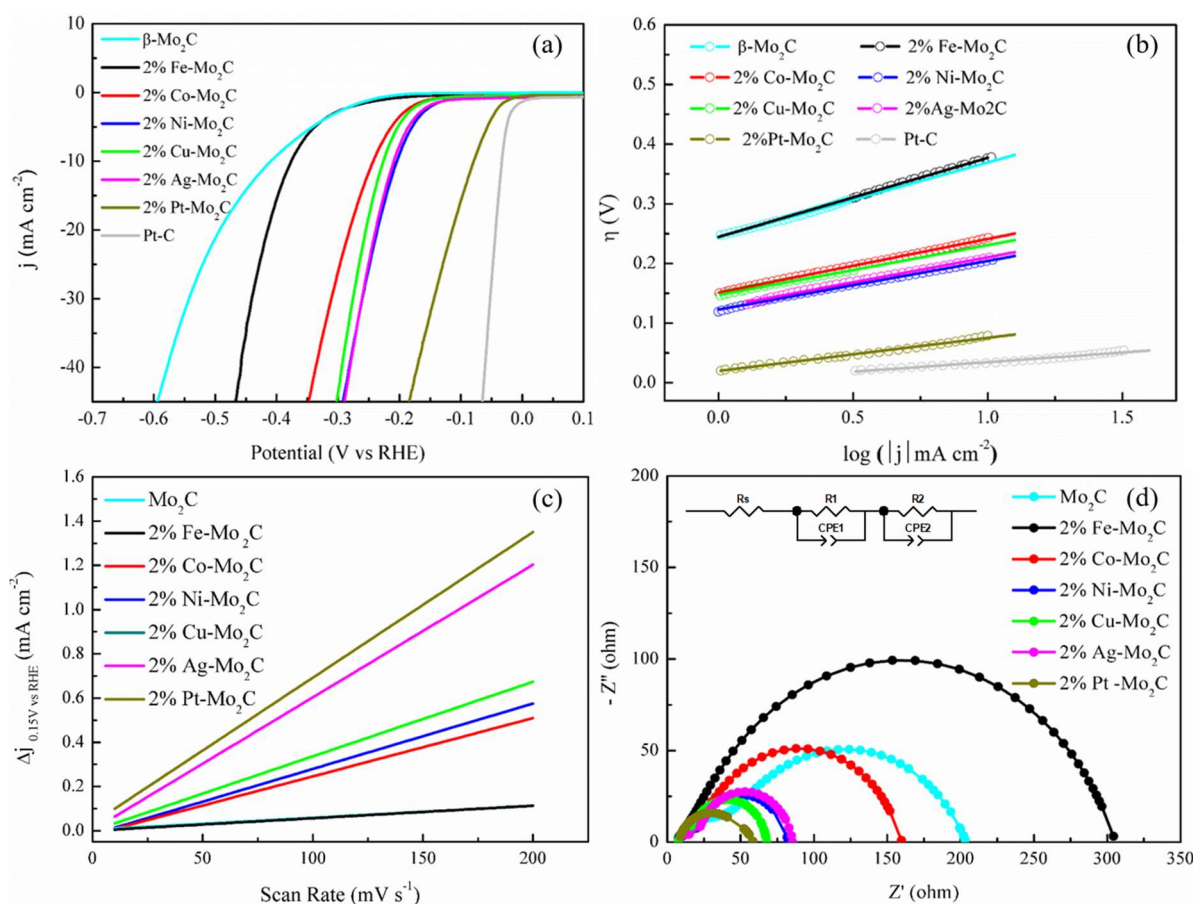


Figure 5. (a) Polarization curves of various metal doped molybdenum carbide catalysts and β -Mo₂C and (b) Tafel plots for HER on modified with GCEs comprising various metal doped molybdenum carbides, pure β -Mo₂C, and commercial 20% Pt/C. (c) Estimation of C_{dl} by plotting the current density variation ($\Delta j = (j_a - j_c)/2$, at 150 mV versus RHE; data obtained from the CV in Figure 6) against scan rate to fit a linear regression, and (d) Nyquist plots (at $\eta = 200$ mV) of the above carbide electrocatalysts.

Table 3. Summary of the HER activity of pure β -Mo₂C and various metal doped molybdenum carbide catalysts in 0.5 M H₂SO₄.

Catalyst	η_{10} (mV)	η_{onset} (mV)	Tafel Slope (mV/dec)	R_{ct} ^(a) (Ω)	C_{dl} ^(b) (mF/cm ²)	j_0 ^(c) (mA/cm ²)
Mo ₂ C	410	245	124	148.40	0.54	1.1×10^{-2}
2% Fe-Mo ₂ C	377	226	132	290.90	0.56	1.4×10^{-2}
2% Co-Mo ₂ C	243	150	89	129.90	2.63	2.0×10^{-2}
2% Ni-Mo ₂ C	205	120	81	64.04	2.96	2.8×10^{-2}
2% Cu-Mo ₂ C	227	146	84	52.33	3.37	1.7×10^{-2}
2% Ag-Mo ₂ C	210	108	83	61.73	6.00	3.0×10^{-2}
2% Pt-Mo ₂ C	79	32	55	54.19	6.59	4.4×10^{-1}
20% Pt/C	34	23	32	\	28.2	8.5×10^{-1}

^(a) Data were measured at $\eta = 200$ mV; ^(b) Data were calculated according to the CV results (Figure 6); ^(c) Exchange current densities (j_0) were obtained from Tafel curves by using extrapolation methods.

Accordingly, the Tafel plots of above catalysts could be divided into two categories in HER kinetics (Figure 5b and Table 3). As compared with pure β -Mo₂C and 2% Fe-Mo₂C, the promoted

kinetic metrics with low onset overpotentials (η_{onset}) and small Tafel slopes (b) are observed on other catalysts. For pure β -Mo₂C and 2% Fe-Mo₂C, 245 mV and 226 mV for onset overpotentials (η_{onset}), and 124 mV/dec and 132 mV/dec for Tafel slopes (b), respectively. When Co, Ni, Cu, and Ag were doped on molybdenum carbide surfaces, the η_{onset} were decreased to 150–110 mV, and the Tafel slopes (b) also decreased to 90–80 mV/dec. Remarkably, the lowest onset overpotentials (η_{onset}) and smaller Tafel slopes (b) are observed on 2% Pt-Mo₂C ($\eta_{\text{onset}} = 32$ mV, $b = 55$ mV/dec) catalyst. The small Tafel slope indicates a fast increase of the hydrogen generation rate with the applied overpotential, corresponding to the high catalytic activity shown in the polarization curves. It is commonly known that HER in acidic aqueous media proceeds in two steps [12,13]. The first step is an electrochemical reduction step (H^+ reduction, Volmer reaction) with a Tafel slope of about -118 mV/dec, and the second one (H_{ads} desorption) is either the ion or atom reaction (Heyrovsky reaction) with a slope of about -40 mV/dec or the atom combination reaction (Tafel reaction) with a slope of 30 mV/dec [22]. Based on the results, one can see that the high Tafel slopes on pure β -Mo₂C and 2% Fe-Mo₂C suggest a rate-determining step of the H^+ reduction (Volmer reaction). However, compared with β -Mo₂C and 2% Fe-Mo₂C, low Tafel slopes were obtained for other metal doped molybdenum carbide catalysts. This indicates that for Co, Ni, Cu, Ag, and Pt doped molybdenum carbide catalysts, the rate-determining step is H_{ads} desorption. These results suggest that the HER kinetics on the molybdenum carbide-based catalyst surface could be influenced by doping of transition metal on its surface.

Extrapolating the above Tafel plot (see in Figure 5b), the calculated exchange current density (j_0) can be used to show the most inherent HER activity (as show in Table 3). The j_0 of 4.4×10^{-1} mA/cm² on 2% Pt-Mo₂C is obviously higher than those of β -Mo₂C (1.1×10^{-2} mA/cm²), 2% Fe-Mo₂C (1.4×10^{-2} mA/cm²), 2% Co-Mo₂C (2.0×10^{-2} mA/cm²), 2% Ni-Mo₂C (2.8×10^{-2} mA/cm²), 2% Cu-Mo₂C (1.7×10^{-2} mA/cm²), and 2% Ag-Mo₂C (3.0×10^{-2} mA/cm²). This result indicates that the intrinsic activity of as-prepared 2% Pt-Mo₂C is higher than the others.

As shown in Figure 5c and d, the electrochemical surface area (ECSA) and resistant charge transfer (R_{ct}) were further measured. Here, ECSA was calculated based on double-layer capacitances (C_{dl}) and the capacity behavior of the catalyst. However, the capacity behavior of molybdenum carbide is still unclear based on our knowledge. Therefore, the accurate measurement of ECSA of as-prepared catalyst cannot be determined directly by using electrochemical methods. An alternative calculation of double-layer capacitances (C_{dl}) was herein employed, which is proportional to ECSA and provides a relative comparison. Derived from the cyclic voltammograms (CVs) versus scan rate in 0.5 M H₂SO₄ (as shown in Figure 6), the C_{dl} of 28.2 mF/cm² was detected for 20% Pt/C catalyst. However, the C_{dl} of 6.59 mF/cm² on 2% Pt-Mo₂C is higher than those on β -Mo₂C (0.54 mF/cm²), 2% Fe-Mo₂C (0.56 mF/cm²), 2% Co-Mo₂C (2.63 mF/cm²), 2% Ni-Mo₂C (2.96 mF/cm²), 2% Cu-Mo₂C (3.37 mF/cm²) and 2% Ag-Mo₂C (6.0 mF/cm²), as shown in Figure 5c and Table 3. The high C_{dl} value implies enriched active sites on 2% Pt-Mo₂C catalyst surface for HER. Furthermore, their electrochemical impedance spectroscopy measurements (Figure 5d) show the order in R_{ct} , in which compared with other metals (e.g., Fe, Co, Ni, Cu and Ag) and pure molybdenum carbide, a R_{ct} as low as 54.19 Ω delivered by 2% Pt-Mo₂C suggests rapid electron transport for hydrogen evolution. This result is consistent with the above experimental result.

Based on the above characterization and electrochemical measurement, it can be deduced that comparing with β -Mo₂C and other metals (Fe, Co, Ni, Cu, Ag) doped molybdenum carbide catalysts, the high HER catalytic activity of 2% Pt-Mo₂C catalyst might be due to its large surface area, large metal dispersion, higher double-layer capacitances (C_{dl}) and more catalytically active sites. On the other hand, based on the Mo 3d XPS profiles (Figure 2 and Table 1), enriched electrons around Mo²⁺ (Mo₂C) can be seen that the after an effective metal-doping, especially for Pt-doping (Mo²⁺ binding energy is 228.6 and 228.0 for β -Mo₂C and 2% Pt-Mo₂C, respectively). Considering the strong hydrogen binding on Mo₂C [27], the excessive electrons in Mo would transfer to the anti-bonding orbitals of Mo-H, resulting in relatively moderate Mo-H for promoting H_{ads} desorption and further increasing

HER activity. Comparing with Tafel slopes in β -Mo₂C (124 mV/dec), the obviously reduced Tafel slope in 2% Pt-Mo₂C (55 mV/dec), indicates accelerated HER kinetics by Pt-doping.

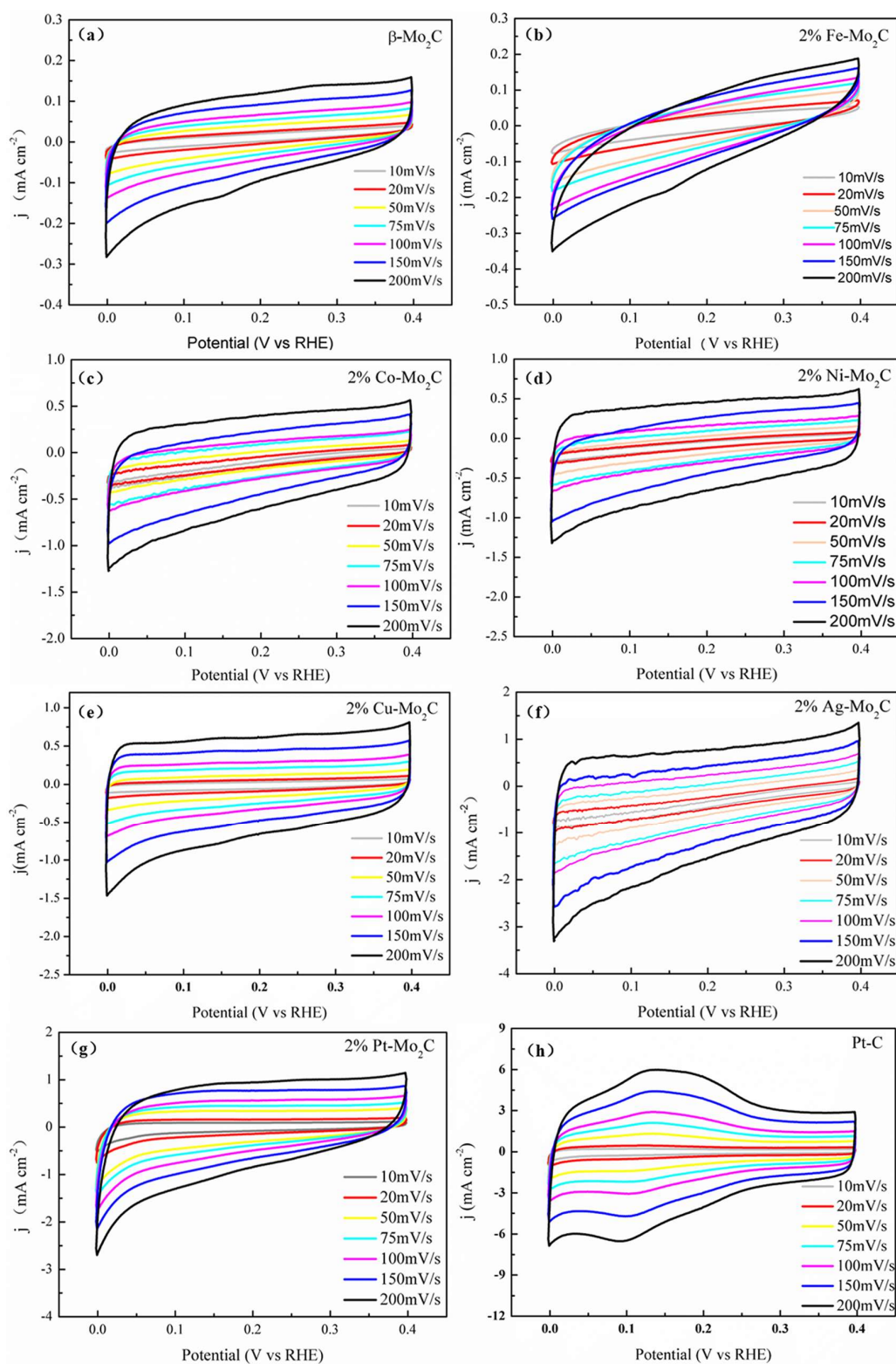


Figure 6. Cyclic voltammograms of (a) β -Mo₂C; (b) 2% Fe-Mo₂C; (c) 2% Co-Mo₂C; (d) 2% Ni-Mo₂C; (e) 2% Cu-Mo₂C; (f) 2% Ag-Mo₂C; (g) 2% Pt-Mo₂C and (h) commercial Pt/C with various scan rates in 0.5 M H₂SO₄.

Another important criterion for a good electrocatalyst is its stability. The long-term stability of 2% Pt-Mo₂C was examined using continuously cycling for 3000 cycles in 0.5 M H₂SO₄ aqueous medium, as shown in Figure 7. One can see that at the end of the cycles, the catalyst affords a similar *j*-V curve to the initial cycle with negligible loss of the cathodic current. The above results confirm the excellent stability in acidic electrolyte.

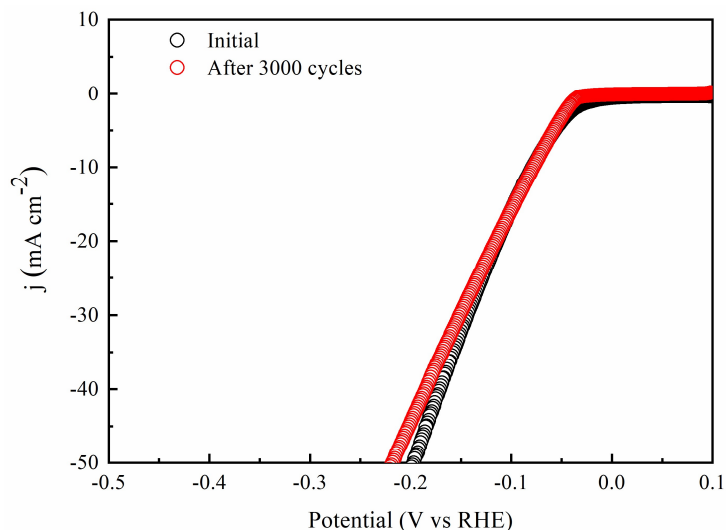


Figure 7. Stability of the 2% Pt-Mo₂C modified electrode with an initial polarization curve and after 3000 cycles in 0.5 M H₂SO₄.

3. Materials and Methods

3.1. Catalyst Preparation

The metal (M) doped MoO_x/organic precursors (M: Fe, Co, Ni, Cu, Ag, and Pt) were prepared as follows: firstly, 2.48 g of ammonium heptamolybdate ((NH₄)₆Mo₇O₂₄·4H₂O; Aladdin Co., 99%, (Shanghai, China)) was dissolved in 40 mL of distilled water at room temperature, and followed by introduction of transition metal precursors ((Fe(NO₃)₃·9H₂O, Aladdin Co., 99%; Co(NO₃)₂·6H₂O, Aladdin Co., 99%; Ni(NO₃)₂·6H₂O, Aladdin Co., 99%; Cu(NO₃)₂·3H₂O, Aladdin Co., 99%; AgNO₃, Aladdin Co., 99% and H₂PtCl₆·6H₂O Aladdin Co., 99%, (Shanghai, China)) The molar ratio of M to (M + Mo) was 2%. The mixed aqueous solution was stirred at room temperature for 30 min, and then 3.28 mL of aniline (C₆H₇N; Macklin Co., AR, (Shanghai, China)) was dropwise added into the above solution. Thereafter, 1 M HCl aqueous solution was added to adjust the pH level to 2–4. The mixed solution was continually stirred at room temperature for 30 min, and then the above mixed solution was heated in an oil bath. After a reaction at 50 °C for 4 h, the obtained precipitate was washed with ethanol and distilled water until the pH value was 7, and then dried at 50 °C overnight. Such solids were transferred into a fixed-bed quartz micro-reactor with an inner diameter of 10 mm. Firstly, air in the reactor was purged out Ar (100 mL/min) at room temperature (25 °C) for 1 h, and then heated to the final carburization temperature (800 °C) with a ramping rate of 2 °C/min in an Ar atmosphere and a flow rate of 50 mL/min, and remained at the final temperature for 5 h. As-obtained catalyst was cooled down to room temperature in the Ar flow and finally passivated in 1% O₂/Ar for 12 h at room temperature. The final products were denoted as 2% M-Mo₂C (M: Fe, Co, Ni, Cu, Ag and Pt).

For comparison, the commercial HER catalyst of 20%Pt/C (Macklin) was used.

3.2. Characterization

Crystal structures of the as-prepared catalysts were determined by X-ray diffraction (D8, Bruker, Germany). The radiation used was Cu K α with an operating potential of 30 kV, a current of 30 mA,

and the scanning rate of 4 deg/min; phase identification was achieved through comparison of XRD patterns to those of the Joint Committee on Powder Diffraction Standards (JCPDS). The surface structure of the catalyst was analyzed by using a transmission electron microscope (TEM; JEM-2100F, JEOL, Tokyo, Japan) operating at 300 kV. Scanning electron microscope (SEM) image was obtained using a JEOL Field Emission Scanning Electron Microscope, (JSM-7500F, JEOL, Tokyo, Japan). The catalyst surface chemical situation was analyzed by using X-ray photoelectron spectroscopy (XPS, Escalab 250Xi, Thermo Fisher Scientific Co., Waltham, MA, USA), using Al K α radiation ($h\nu = 1486.6$ eV) as the photon source, generation at 150 W, and using C 1s (284.6 eV) as a reference. The binding energies of Mo 3d were analyzed by using the Shirley baseline correction. Brunauer-Emmett-Teller (BET, Tristar II Plus, Micromeritics, Atlanta, USA) surface area was measured through nitrogen adsorption at 77 K, using a Micromeritics Tristar II Plus automatic absorption instrument. The doped metal (Fe, Co, Ni, Cu, Ag, and Pt) and Mo contents of M-Mo₂C nanowires were determined by inductively coupled plasma (ICP, Thermo ICAP RQ, Waltham, MA, USA).

3.3. Electrode Preparation and Its Performance Test for HER

The 2% M-Mo₂C (M: Fe, Co, Ni, Cu, Ag and Pt) catalysts were loaded onto a glassy carbon electrode (GCE) for testing in 0.5 M H₂SO₄ solution using a typical three-electrode setup. Typically, 4 mg of as-prepared catalyst and 40 μ L of 5 wt% Nafion solution were dispersed in 1 mL of 4:1 *v/v* water/ethanol by 30 min sonication to form a homogeneous ink. Then 5 μ L of catalyst ink was loaded onto a GCE of 3 mm in diameter. As such, the catalyst loading amount was 0.272 mg/cm². Finally, the as-prepared electrode was dried at room temperature for 30 min. Linear sweep voltammetry was conducted with a scan rate of 2 mV/s on a potentiostat of CHI 760 (CH Instruments, Shanghai, China), using an Ag/AgCl/saturated KCl as the reference electrode, and a graphite electrode as the counter electrode. All the potentials reported in this study were referenced to a reversible hydrogen electrode (RHE) by adding a value of (0.198 + 0.059 pH) V.

4. Conclusions

In summary, HER was performed on various transition metals (Fe, Co, Ni, Cu, Ag, and Pt) doped on molybdenum carbides by an organic-inorganic precursor carburization process. Comparing with the undoped molybdenum carbide, metal doped molybdenum carbides showed higher electrocatalytic activity for HER. Especially, Pt doped molybdenum carbide (2% Pt-Mo₂C) showed the highest catalytic performance (catalytic activity and stability in 0.5 M H₂SO₄) among the prepared metal doped catalysts. The highly catalytic performance of 2% Pt-Mo₂C is due to its high surface area, high metal dispersion, electron transfer, and more active sites. Although the catalyst with the highest activity in this report is still using Pt as the main composition for HER, the ultra-low loading amount (comparing with the commercial 20% Pt/C) and high earth-abundance of Mo metal highlight its promising prospect as a highly efficient electrocatalyst. Based on the XPS, SEM, BET, and electrochemical properties results, the surface physicochemical properties of molybdenum carbide could be influenced by the doping-metal. This work is expected to open up a new opportunity to develop lower cost catalysts with high-performance via engineering on composition, nanostructure, and surface state.

Author Contributions: Conceptualization, Y.M.; Methodology, Y.M.; Software, M.C., Y.Z. and C.L.; Formal Analysis, Y.M. and Y.Q.; Investigation, Y.M.; Resources, Y.M. and Z.Z.; Writing-Review and Editing, G.G. and X.L.; Visualization, Y.M. and M.C.; Supervision, Y.M. and Y.F.; Project Administration, Y.M. and T.W.

Funding: This research was funded by [National Natural Science Foundation of China] grant number [51701046], [Natural Science Foundation of Guangdong Providence] grant number [2017A030310333], and [Educational Commission of Guangdong Province] grant number [2016KQNCX044].

Acknowledgments: The authors thank Zhan Li's Group especially Chao Chen for their help with the BET measurements. The authors would also like to thank Chengchao Li and Hongbo Geng for the conversations about the electrochemistry. Z.S. Zhang is thankful to the Shandong Provincial Natural Science Foundation (no. ZR2016BB27).

Conflicts of Interest: The authors declare no conflict of interest. The funders had no role in the design of the study; in the collection, analyses, or interpretation of data; in the writing of the manuscript, and in the decision to publish the results.

References

1. Chen, W.; Pei, J.; He, C.T.; Wan, J.; Ren, H.; Zhu, Y.; Wang, Y.; Dong, J.; Tian, S.; Cheong, W.C.; et al. Rational design of single molybdenum atoms anchored on N-doped carbon for effective hydrogen evolution reaction. *Angew. Chem. Int. Edit.* **2017**, *56*, 16086–16090. [[CrossRef](#)] [[PubMed](#)]
2. Ma, Y.; Guan, G.; Hao, X.; Cao, J.; Abudula, A. Molybdenum carbide as alternative catalyst for hydrogen production—a review. *Renew. Sust. Energ. Rev.* **2017**, *75*, 1101–1129. [[CrossRef](#)]
3. Mahmood, J.; Li, F.; Jung, S.M.; Okyay, M.S.; Ahmad, I.; Kim, S.J.; Park, N.; Jeong, H.Y.; Baek, J.B. An efficient and pH-universal ruthenium-based catalyst for the hydrogen evolution reaction. *Nat. Nanotechnol.* **2017**, *12*, 441–446. [[CrossRef](#)] [[PubMed](#)]
4. Lin, L.; Zhou, W.; Gao, R.; Yao, S.; Zhang, X.; Xu, W.; Zheng, S.; Jiang, Z.; Yu, Q.; Li, Y.W.; Shi, C.; Wen, X.D.; Ma, D. Low-temperature hydrogen production from water and methanol using Pt/ α -MoC catalysts. *Nature* **2017**, *544*, 80–83. [[CrossRef](#)] [[PubMed](#)]
5. Yarlagadda, V.; Carpenter, M.K.; Moylan, T.E.; Kukreja, R.S.; Koestner, R.; Gu, W.; Thompson, L.; Kongkanand, A. Boosting fuel cell performance with accessible carbon mesopores. *ACS Energy Lett.* **2018**, *3*, 618–621. [[CrossRef](#)]
6. Yao, S.; Zhang, X.; Zhou, W.; Gao, R.; Xu, W.; Ye, Y.; Lin, L.; Wen, X.; Liu, P.; Chen, B.; et al. Atomic-layered Au clusters on α -MoC as catalysts for the low-temperature water-gas shift reaction. *Science* **2017**, *357*, 389–393. [[CrossRef](#)] [[PubMed](#)]
7. Ma, Y.; Guan, G.; Phanthong, P.; Hao, X.; Huang, W.; Tsutsumi, A.; Kusakabe, K.; Abudula, A. Catalytic activity and stability of nickel-modified molybdenum carbide catalysts for steam reforming of methanol. *J. Phys. Chem. C* **2014**, *118*, 9485–9496. [[CrossRef](#)]
8. Ma, Y.; Guan, G.; Hao, X.; Zuo, Z.; Huang, W.; Phanthong, P.; Li, X.; Kusakabe, K.; Abudula, A. Embedded structure catalyst: A new perspective from noble metal supported on molybdenum carbide. *RSC Adv.* **2015**, *5*, 15002–15005. [[CrossRef](#)]
9. Cao, J.; Ma, Y.; Guan, G.; Hao, X.; Ma, X.; Wang, Z.; Kusakabe, K.; Abudula, A. Reaction intermediate species during the steam reforming of methanol over metal modified molybdenum carbide catalysts. *Appl. Catal. B* **2016**, *189*, 12–18. [[CrossRef](#)]
10. Ma, Y.; Guan, G.; Hao, X.; Zuo, Z.; Huang, W.; Phanthong, P.; Kusakabe, K.; Abudula, A. Highly-efficient steam reforming of methanol over copper modified molybdenum carbide. *RSC Adv.* **2014**, *4*, 44175–44184. [[CrossRef](#)]
11. Cook, T.R.; Dogutan, D.K.; Reece, S.Y.; Surendranath, Y.; Teets, T.S.; Nocera, D.G. Solar energy supply and storage for the legacy and nonlegacy worlds. *Chem. Rev.* **2010**, *110*, 6474–6502. [[CrossRef](#)] [[PubMed](#)]
12. Jahan, M.; Liu, Z.; Loh, K.P. A graphene oxide and copper-centered metal organic framework composite as a tri-functional catalyst for HER, OER, and ORR. *Adv. Funct. Mater.* **2013**, *23*, 5363–5372. [[CrossRef](#)]
13. Li, Y.; Wang, H.; Xie, L.; Liang, Y.; Hong, G.; Dai, H. MoS₂ nanoparticles grown on graphene: an advanced catalyst for the hydrogen evolution reaction. *J. Am. Chem. Soc.* **2011**, *133*, 7296–7299. [[CrossRef](#)] [[PubMed](#)]
14. Cheng, N.; Stambula, S.; Wang, D.; Banis, M.N.; Liu, J.; Riese, A.; Xiao, B.; Li, R.; Sham, T.K.; Liu, L.M.; et al. Platinum single-atom and cluster catalysis of the hydrogen evolution reaction. *Nat. Commun.* **2016**, *7*, 13638. [[CrossRef](#)] [[PubMed](#)]
15. Yang, Y.; Lun, Z.; Xia, G.; Zheng, F.; He, M.; Chen, Q. Non-precious alloy encapsulated in nitrogen-doped graphene layers derived from MOFs as an active and durable hydrogen evolution reaction catalyst. *Energy Environ. Sci.* **2015**, *8*, 3563–3571. [[CrossRef](#)]
16. Lee, J.S.; Yeom, M.H.; Park, K.Y.; Nam, I.S.; Chung, J.S.; Kim, Y.G.; Moon, S.H. Preparation and benzene hydrogenation activity of supported molybdenum carbide catalysts. *J. Catal.* **1991**, *128*, 126–136. [[CrossRef](#)]
17. Porosoff, M.D.; Yang, X.; Boscoboinik, J.A.; Chen, J.G. Molybdenum carbide as alternative catalysts to precious metals for highly selective reduction of CO₂ to CO. *Angew. Chem. Int. Ed.* **2014**, *53*, 6705–6709. [[CrossRef](#)] [[PubMed](#)]

18. Zhang, X.; Zhu, X.; Lin, L.; Yao, S.; Zhang, M.; Liu, X.; Wang, X.; Li, Y.W.; Shi, C.; Ma, D. Highly dispersed copper over β -Mo₂C as an efficient and stable catalyst for the reverse water gas shift (RWGS) reaction. *ACS Catal.* **2017**, *7*, 912–918. [[CrossRef](#)]
19. Blekkan, E.A.; Pham-Huu, C.; Ledoux, M.J.; Guille, J. Isomerization of n-heptane on an oxygen-modified molybdenum carbide catalyst. *Ind. Eng. Chem. Res.* **1994**, *33*, 1657–1664. [[CrossRef](#)]
20. Liao, L.; Wang, S.; Xiao, J.; Bian, X.; Zhang, Y.; Scanlon, M.D.; Hu, X.; Tang, Y.; Liu, B.; Girault, H.H. A nanoporous molybdenum carbide nanowire as an electrocatalyst for hydrogen evolution reaction. *Energy Environ. Sci.* **2014**, *7*, 387–392. [[CrossRef](#)]
21. Vrubel, H.; Hu, X. Molybdenum boride and carbide catalyze hydrogen evolution in both acidic and basic solutions. *Angew. Chem.* **2012**, *124*, 12875–12878. [[CrossRef](#)]
22. Lin, H.; Liu, N.; Shi, Z.; Guo, Y.; Tang, Y.; Gao, Q. Cobalt-doping in molybdenum-carbide nanowires toward efficient electrocatalytic hydrogen evolution. *Adv. Funct. Mater.* **2016**, *26*, 5590–5598. [[CrossRef](#)]
23. Wang, J.; Cao, J.; Ma, Y.; Li, X.; Xiaokaiti, P.; Hao, X.; Yu, T.; Abudula, A.; Guan, G. Decomposition of formic acid for hydrogen production over metal doped nanosheet-like MoC_{1-x} catalysts. *Energy Convers. Manag.* **2017**, *147*, 166–173. [[CrossRef](#)]
24. Cao, J.; Wang, J.; Ma, Y.; Li, X.; Xiaokaiti, P.; Hao, X.; Abudula, A.; Guan, G. Hydrogen production from formic acid over morphology-controllable molybdenum carbide catalysts. *J. Alloys Compd.* **2018**, *735*, 1463–1471. [[CrossRef](#)]
25. Wang, Y.; Shi, Z.; Mo, Q.; Gao, B.; Liu, B.; Wang, L.; Zhang, Y.; Gao, Q.; Tang, Y. Mesoporous and skeletal molybdenum carbide for hydrogen evolution reaction: diatomite-type structure and formation mechanism. *Chem. Electro. Chem.* **2017**, *4*, 2169–2177. [[CrossRef](#)]
26. Wan, C.; Regmi, Y.N.; Leonard, B.M. Multiple phases of molybdenum carbide as electrocatalysts for the hydrogen evolution reaction. *Angew. Chem.* **2014**, *126*, 6525–6528. [[CrossRef](#)]
27. Michalsky, R.; Zhang, Y.J.; Peterson, A.A. Trends in the hydrogen evolution activity of metal carbide catalysts. *ACS Catal.* **2014**, *4*, 1274–1278. [[CrossRef](#)]



© 2018 by the authors. Licensee MDPI, Basel, Switzerland. This article is an open access article distributed under the terms and conditions of the Creative Commons Attribution (CC BY) license (<http://creativecommons.org/licenses/by/4.0/>).